AIAA JOURNAL
Vol. 44, No. 10, October 2006

Sensing Flow Separation on a Circular Cylinder by Micro-Electrical-Mechanical-System Thermal-Film Sensors

J. J. Miau,* J. K. Tu,† J. H. Chou,‡ and G. B. Lee‡
National Cheng-Kung University, Tainan 701, Taiwan, Republic of China

DOI: 10.2514/1.17408

Unsteady characteristics of flow separation from a circular cylinder, at Reynolds numbers of 1.65–1.71 × 10^4, were studied using Wavelet analysis of the signals obtained by a micro-electrical-mechanical-system film sensors array flushed with the cylinder surface. At $\theta = 85$ deg near where flow separation took place, it was found that the unsteady flow behaviors were featured with two time scales, one of which was associated with vortex shedding, and the other was at least 1 order of magnitude longer due to excursion of flow separation in a circumferential region of the extent about 5 deg. The Wavelet analysis results enabled one to reduce the percentage of time during which the vortex shedding frequency was detectable at the location measured. In the region upstream of flow separation the percentage values obtained were very close to 100%, followed by a pronounced decrease from $\theta = 85$ to 100 deg. At $\theta = 100$ deg, the percentage values reduced were about 30%. Moreover, low-frequency modulations were noticed in the signals measured by the thermal-film sensors situated upstream of flow separation and the hot-wire in the freestream. The Wavelet analysis with these signals revealed a trend that the lower the vortex shedding frequency, the larger the amplitude of the vortex shedding frequency component.

Introduction

Studying flow separation from a circular cylinder using thermal-film sensors can be traced to the works of Giedt [1] and Bellhouse and Schultz [2]. Bellhouse and Schultz employed a thin platinum film on a circular cylinder to measure the skin friction at Reynolds numbers of 10^4–10^5. In this study, a theoretical analysis of heat transfer of a two-dimensional thermal film subjected to steady and unsteady boundary-layer flows was performed. As they found, when the frequency parameter $\omega L/U_0$ was significant, the unsteady heat transfer rate and the skin friction on the wall might no longer be in phase, where ω, L, and U_0 were denoted the characteristic frequency of the unsteady flow, the streamwise length of the film, and the freestream velocity of the boundary layer, respectively. Later, Dwyer and McCroskey [3] employed a thermal film flushed with the surface of a circular cylinder to measure the shear stress on the surface up to the point of separation. They pointed out that the separation point was actually moving on the cylinder, and the data reduced from a film sensor could infer the minimum angle from the forward stagnation point corresponding to the onset of separation and the maximum angle beyond which the flow was always separated. The behavior of flow separation was further confirmed by the velocity measurements with a double hot-wires probe situated slightly above the surface of the cylinder. Comparing the output signals of the two hot wires enabled one to clarify the status of flow reversal and identify the region where the instantaneous zero wall shear took place. Blevins [4] employed a circular cylinder with 13 flush-mounted film sensors, nine of which were arranged along the spanwise direction evenly spaced. As the film sensors were situated upstream of the flow separation point, the fluctuations of the signals were dominated by the vortex shedding frequency component, which were seen not in phase always. Moreover, each signal trace appeared to consist of amplitude-modulated vortex shedding cycles, whose vortex shedding frequencies wandered 1–2% with respect to time. He further noted a trend that the larger the fluctuating amplitude, the lower the frequency of vortex shedding. Recently, Lee [5] applied multiple hot-film sensors on a circular cylinder, enabling simultaneous measurements of unsteady flow characteristics upstream and downstream of flow separation. Undulations of the vortex shedding frequency component measured upstream and downstream of flow separation appeared in an antiphase manner. Moreover, the signals measured in the neighborhood of flow separation point were characterized by two times the vortex shedding frequency. This was reasoned due to the separation point passing over the sensor twice during a cycle of vortex shedding. The thermal-film array employed by Lee [5] consisted of thin nickel films (0.2 μm) which were electron-beam evaporated onto a thin polyimide substrate (50 μm). Liu and Brodie [6] employed four micro-electrical-mechanical-system (MEMS) sensor arrays, each of which consisted of 32 polysilicon hot-wire sensors, spanning over a circumferential region of 0–180 deg on a circular cylinder. The signals of the multiple sensors measured revealed the flow characteristics similar to those described by Lee [5]. Liu and Brodie [6] further manipulated control of flow instability by external disturbances at frequencies of one order greater than the vortex shedding frequency.

The present study was motivated by a recent work performed in a water channel concerning flow separation from a circular cylinder. For illustration, six photos obtained by flow visualization at every 0.2 s, for $Re = 1.8 \times 10^4$, are presented in Fig. 1. In this case, the vortex shedding period was about 1 s. The dye was released from the cylinder surface at $\theta = 70$ deg, where $\theta = 0$ denoted the forward stagnation point of the flow; thus the dye was able to convect downstream very near the wall. It is seen in each of the photos that the dye was accumulated in the neighborhood of $\theta = 85$ deg, signifying the occurrence of flow separation. Despite that the criteria of unsteady separation [7–10] caution one to make further interpretations of the photos in Fig. 1, these photos definitely unveil the unsteady, three-dimensional nature of the flow separation phenomenon. Motivated by the flow visualization results obtained, the present study was aimed to gain further understandings on the flow separation phenomenon using self-made MEMS thermal-film sensors. To accomplish this task, the thermal-film sensor signals were analyzed with a Wavelet analysis technique to resolve the spectral contents of the signals to local time. Previous experiences

Presented as Paper 0299 at the 43rd Aerospace Sciences Meeting & Exhibit, Reno, Nevada, 10–13 January 2005; received 25 May 2005; revision received 2 December 2005; accepted for publication 20 March 2006.

*Department of Aeronautics and Astronautics; jjmiau@mail.ncku.edu.tw.
†Department of Aeronautics and Astronautics.
‡Department of Engineering Science.

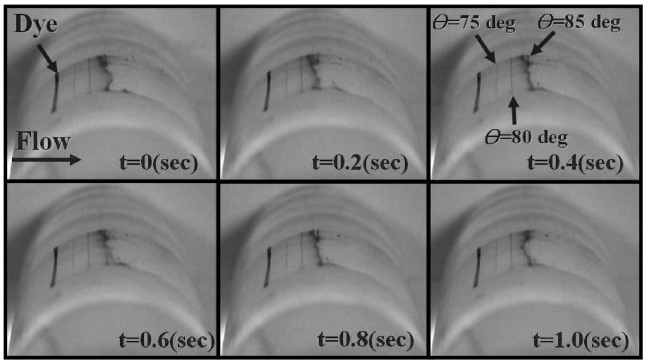

Fig. 1 Flow visualization photos taken in an experiment of flow over a circular cylinder in a water-channel facility.

[11,12] indicate that this technique was very useful to provide the information concerning the instantaneous behavior of unsteady flow.

Experimental Methods

Experiments were carried out in a low-speed wind tunnel, whose test section was 150 by 160 mm in cross section. In the test section, the maximum velocity measured was about 20 m/s, at which the freestream turbulence intensity measured was less than 0.5%. The circular cylinder employed for the present study was 32 mm in diameter and 160 mm in length. The cylinder spanned the two sidewalls of the test section. Shown in Fig. 2a is a schematic drawing of the present flow configuration and the coordinate system employed. $\theta = 0$ denotes the forward stagnation point of flow over the circular cylinder. This point was determined by examining the FFT spectrum of the thermal-film signals obtained, of which two peak frequencies, i.e., the vortex shedding frequency and its harmonic, were clearly identified [5,6].

In the present study, the Reynolds number, Re, is defined based on the diameter of the cylinder, D, and the incoming velocity, U_0, The experimental data reported here were obtained at $Re = 1.65$–1.71×10^4, which fall in the regime of laminar flow separation from a circular cylinder [13].

Figure 2b shows the design of MEMS sensors on a flexible skin. The MEMS thermal films were made of platinum 0.1 μm in thickness, deposited on a polyimide substrate as the flexible skin. The thickness of the polyimide substrate is less than 10 μm. Thus, the presence of the MEMS sensors on the cylinder surface would cause negligible impact on surface smoothness, aerodynamically speaking. There were eight sensors aligned circumferentially on the cylinder, every 5 deg equally spaced. Each of the thermal-film sensors was characterized by a resistance about 200 ohms at room temperature with the temperature coefficient of resistance 0.00247/°C. Each sensor was integrated in a Wheatstone bridge, which was connected to a constant voltage power supply at 5 V. The sensor output sensitivity was about 70 mV/°C when operated with an electric current at 7 mA. Literally speaking, a thermal-film sensor flushed with the surface senses flow motion, because of heat transfer between the heated film and the flow. Heat loss from a thermal film can be related to the magnitude of local shear stress of the flow [2], but not the direction of the flow.

Apart from the MEMS sensors on the cylinder surface, a hot-wire probe was placed in the freestream for monitoring fluctuating motions due to convection of shedding vortices. A photo shown in Fig. 2c illustrates the experimental setup with the circular cylinder and a normal hot-wire probe located at $(x, y, z) = (1D, 1D, 0)$. The velocity measurements obtained by the hot wire served as a reference for comparing with the data reduced from the thermal-film sensors.

In this study, the signals obtained by the thermal-film sensors and the hot wire were sampled at 20 KHz per channel, unless mentioned otherwise. This sampling rate was chosen to satisfy the frequency resolution requirement of the Wavelet analysis results. For the present Wavelet analysis, a Morlet wavelet function was adopted

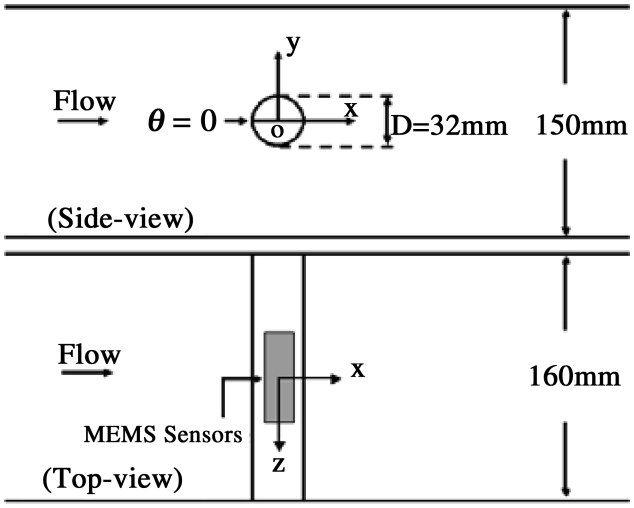

a)

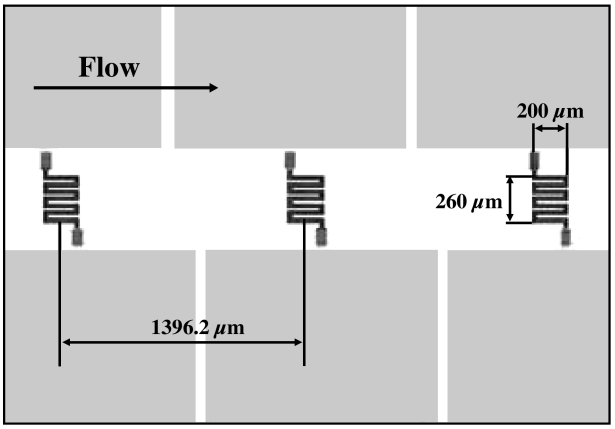

b)

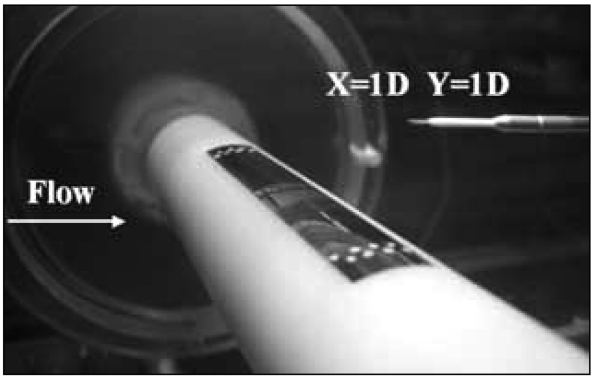

c)

Fig. 2 a) Schematic drawing of the coordinate system employed, b) design of the MEMS sensors, and c) photo showing a hot-wire probe with the MEMS sensors.

[11,12]. More information of Wavelet analysis and its applications in fluid mechanics can be found in Farge [14].

Results and Discussion

General Considerations of the Thermal-Film Signals Measured

Figure 3 presents the signal traces obtained by seven thermal-film sensors on the cylinder surface and a normal hot wire situated at $(x, y, z) = (1D, 1D, 0)$, within a sampled period of 2 s, at

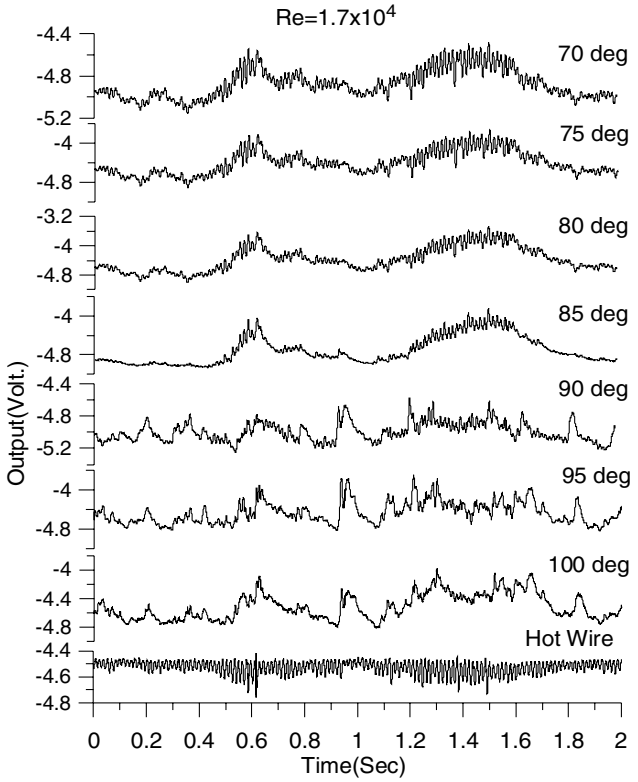

Fig. 3 The output signals of seven thermal-film sensors at $\theta = 70$–100 deg.

$Re = 1.71 \times 10^4$. Pronounced fluctuations are noticed in the signal traces, inferring that the boundary layer developed along the surface of the circular cylinder was highly unsteady, without saying flow downstream in the separation region. According to Bellhouse and Schultz [2] and Menendez and Ramaprian [15], for a film sensor flushed with a surface subjected to a periodically unsteady freestream flow, the shear stress measured would deviate from that reduced in a steady flow, if the unsteady parameters of frequency and amplitude were significant. In the present study, no attempts were made to convert the output voltage of each film sensor to actual shear stress on the surface of the circular cylinder. Therefore, the voltage values of the signals will not be considered for quantitative analysis in the following.

In viewing that the present film sensors were situated on a polyimide substrate, some considerations regarding heat transfer of a sensor together with the substrate subjected to unsteady flows are given here. Bellhouse and Schultz [2] mentioned that for a platinum film of 1 μm in thickness the thermal diffusion time is characterized by 0.04 μs. Because the present film sensor is even thinner, 0.1 μm in thickness, thermal diffusion along the sensor thickness should take negligible amount of time compared with the smallest convection time scale of the present flow. On the other hand, it is a concern that a sensor might respond differently to low and high frequencies of the flow disturbances imposed. At low frequency, temperature change of a sensor would be influenced substantially by the substrate, because the substrate temperature is changing as well. At high frequency, the thermal inertia of the substrate would appear so large that its temperature change is rather insignificant; therefore the sensor output would be mainly due to the temperature change of the sensor. Breuer [16] addressed that the dynamic response of a shear stress sensor could be improved with a design of having a cavity below a nitride

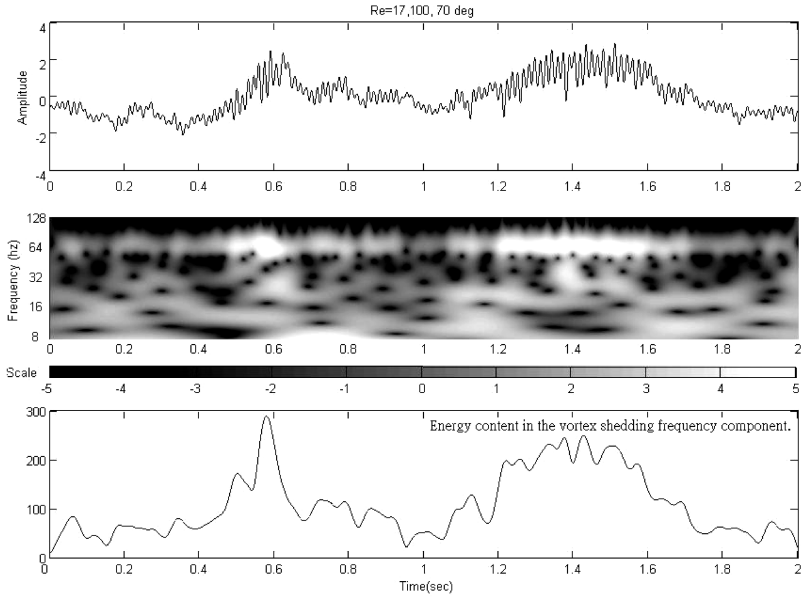

a)

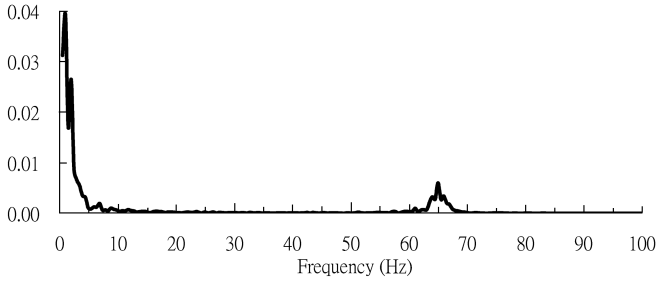

b)

Fig. 4 a) Wavelet spectral distribution and temporal variations of the energy content in the vortex shedding frequency component; b) FFT spectrum.

membrane, on which a platinum sensor was situated. For the sake of simplifying the manufacturing process, the present design of MEMS sensors had platinum film deposited on a polyimide layer.

In Fig. 4a, a Wavelet spectral plot of the MEMS signal trace obtained at $\theta = 70$ deg in Fig. 3 is presented. The merit of this analysis is readily seen that this plot provides a time-frequency spectral distribution of the signals analyzed. Thus, the vortex shedding frequency at a time instant can be resolved from the spectral distribution, the one whose modulus shows a local maximum value. As a result, the vortex shedding frequency obtained by this method, called f_s, would be varying with time. On the other hand, by Fourier transformation, one can identify a peak frequency from a sampled signal trace, which is referred to as the time-mean vortex shedding frequency here, called F_s. For instance, in Fig. 4b the FFT spectrum of the signals trace in Fig. 4a shows that F_s is about 64 Hz.

Also included in Fig. 4a is a plot depicting the temporal variations of the energy content in the vortex shedding frequency component. This quantity at a time instant was reduced by integrating over the Wavelet modulus values within a frequency band of $\pm 10\%$ about F_s. The width of this frequency band was chosen based on our experiences with the signals measured. Normally, such a frequency band would encompass most of the fluctuating energy associated with the vortex shedding frequency component. For instance, the appearance of the frequency spectrum in Fig. 4b confirms this statement.

In the energy content plot in Fig. 4a, one notices that at some instants, for instance, at the time instants 0, 0.17, 0.97, and 1.90 s, the energy content of the vortex shedding frequency component appears significantly lower than that seen at other time instants. In fact, the fluctuating energy could be so low that the identification of the vortex shedding frequency was not possible. An example of this sort is shown in Fig. 5, in which the raw signal traces obtained at $\theta =$ 70–80 deg within a sampled time period $t = 3$–3.5 s, together with

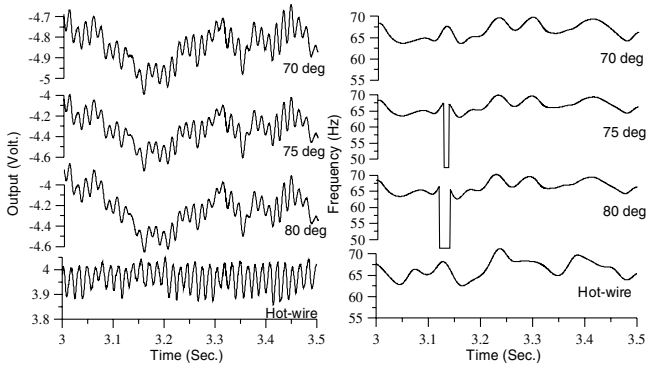

Fig. 5 Referring to the signal traces included, a comparison of the f_s values reduced from the film sensors.

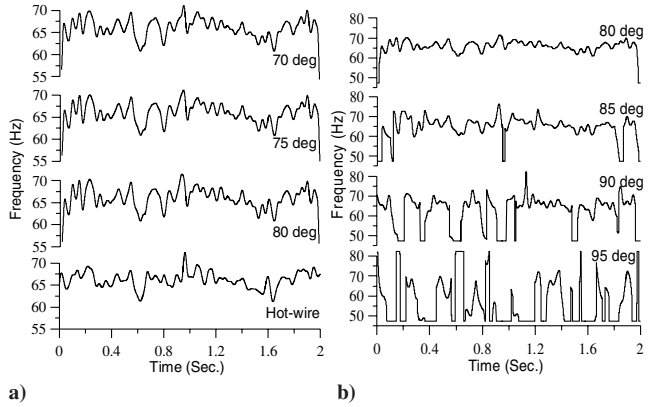

Fig. 6 Temporal variations of the f_s values corresponding to a) the signal traces of $\theta = 70$–80 deg and the hot wire, and b) the signal traces of $\theta = 80$–95 deg.

Table 1 Statistics of the dropout events in finding f_s with the present Wavelet analysis

Initial time instant, s	$T = 0$	$T = 60$	$T = 120$	$T = 180$	$T = 240$
$t = T + 0$	1.94%	0.57%	1.28%	0.34%	1.66%
$t = T + 10$	1.79%	1.06%	0.76%	3.55%	2.74%
$t = T + 20$	0.48%	2.44%	2.14%	1.74%	4.61%
$t = T + 30$	0.59%	0.67%	3.11%	2.28%	1.11%
$t = T + 40$	4.28%	2.51%	0.52%	0.27%	3.14%
$t = T + 50$	1.54%	1.77%	0.59%	2.46%	2.37%

Table 2 Correlation coefficients in every 10 s associated with the f_s values

Time, s	$\theta = 70$–75 deg	$\theta = 70$ deg–hot wire
0–10	0.916	0.722
10–20	0.992	0.729
20–30	0.947	0.805
30–40	0.937	0.635
40–50	0.967	0.590
50–60	0.98	0.741

the f_s values reduced, are presented for discussion. Also included in the figure for reference are the signal trace obtained by the hot-wire probe situated at $(x, y, z) = (1D, 1D, 0)$, and the f_s values reduced. As seen, the f_s values obtained at $\theta = 75$ and 80 deg during $t =$ 3.1–3.2 s are out of range, which appear like dropouts. Within the time period, the Wavelet analysis results actually indicated that significant amount of fluctuating energy was resided in a frequency range which is much lower than F_s. As a result, the present analysis was not able to identify a meaningful vortex shedding frequency. Our experiences indicate that the number of dropout events could be minimized by filtering out low-frequency fluctuations in the raw signals before Wavelet analysis. But, it was not possible to eliminate all the dropout events, due to the nature of the signals measured. For reference, Table 1 shows the statistics of the percentage of time during which the dropout events were found in either the hot-wire signals measured at $(x, y, z) = (1D, 1D, 0)$ or the thermal-film signals measured at $\theta = 70$ deg. Both signals were sampled over a time period of 300 s simultaneously. As seen, the percentage values in every 10 s sampled scatter randomly between 0.3 and 4.6%, based on which the averaged value amounts to 1.81%.

Figure 6 presents temporal variations of the f_s values reduced from the signal traces in Fig. 3, except the one obtained at $\theta = 100$ deg. In Fig. 6a, a comparison of the f_s values obtained at $\theta = 70$, 75, and 80 deg shows that they are nearly identical; on the other hand appreciable discrepancy between these values and those reduced from the hot-wire signal trace is noticed. Further experiment was made with the hot-wire probe positioned very close to the thermal-film sensor at $\theta = 70$ deg. Namely, the hot-wire probe was situated at $(x, y, z) = (-0.125D, 0.563D, 0)$, only 2.4 mm above the film, just outside the boundary layer developed on the surface of the cylinder. The results obtained from this experiment are shown in Table 2, in which the correlation coefficients associated with the f_s values reduced at $\theta = 70$ and 75 deg, and those associated with the f_s values reduced at $\theta = 70$ deg and outside the boundary layer, in every 10 s, are presented. Whereas the coefficients of the former category appears nearly 1, indicating that the f_s values reduced at $\theta = 70$ and 75 deg are nearly identical, the coefficients of the latter category suggest that the f_s values reduced at the cylinder surface be somewhat differed from those reduced outside the boundary layer. Because the hot-wire probe was situated very close to the film sensor in this case, the differences seen are resorted to the nonlinear nature of the boundary-layer flow.

In Fig. 6b, temporal variations of the f_s values reduced at $\theta =$ 80 deg and those at the locations further downstream are differed in appearance. Notably, at $\theta = 85$–95 deg, there is a significant amount of time during which no vortex shedding frequency was identified. This is because the sensors were immersed in the flow separation

region. Further discussion on the characteristics of the thermal-film sensor signals measured in the neighborhood of the flow separation point will be given next.

Unsteady Behaviors of Flow Separation

Referring to earlier reports in the literature [2,3,17], the time-mean flow separation point on a circular cylinder could be determined as the point where the time-mean wall shear stress was vanished. On the other hand, without quantitative information of shear stress on the cylinder surface, Lee [5] and Liu and Brodie [6] were able to address the flow characteristics in the neighborhood of the separation point based on the unsteady behaviors of the sensors signals. An interesting finding reported was that if a film sensor happened to be situated within the traversing range of the separation point, the fluctuations in the signals measured would be dominated by a frequency two times the vortex shedding frequency. These findings stimulated the present study to conduct a detailed examination on the signals measured by the MEMS sensors in the neighborhood of the flow separation point.

Figure 7 presents two signal traces obtained by the MEMS film sensors at $\theta = 80$ and 85 deg, respectively, for $Re = 1.65 \times 10^4$. In reference to the signal trace of $\theta = 80$ deg, the characteristics of the signal trace of $\theta = 85$ deg vary remarkably within a time length of 1 s shown. Specifically speaking, during $t = 0$–0.1 s the two signal traces behave quite alike that the characteristic fluctuations are dominated by the vortex shedding frequency component and appear in phase, inferring that these two locations are immersed in the unsteady boundary layer upstream of flow separation. During $t =$ 0.15–0.3 s, the two signal traces behave differently, that the signal trace of $\theta = 85$ deg appeared to be characterized by the fluctuations at twice the vortex shedding frequency. Referring to Lee [5] and Liu and Brodie [6], these appearances infer a situation that the flow separation point is passing over the measured location twice in a cycle of vortex shedding. During $t = 0.75$–0.85 s, fluctuations in the signal traces of $\theta = 80$ and 85 deg appear to be dominated by the vortex shedding frequency component, but out of phase. Referring to Lee [5] and Liu and Brodie [6], this rather indicates that flow separation takes place between these two sensor locations. Hence, at these moments the flow separation point was situated relatively forward, compared with other time instants shown in the figure.

Having realized the unsteady nature of flow separation, one further examines the signal traces obtained at $\theta = 75$ and 90 deg in Fig. 8, with the signal trace obtained at $\theta = 80$ deg as a reference. Note that the fluctuations shown in these signal traces were normalized by the respective root-mean-square values beforehand. Seen in Fig. 8a is that the signal traces of $\theta = 75$ and 80 deg are almost coincided. This appearance simply infers that these two locations were situated upstream of the flow separation point during the time measured. Moreover, this appearance suggests that the boundary layer developed on the cylinder surface upstream of flow separation be laminar, in which random fluctuations were rarely detected by the sensors. In Fig. 8b, it is seen that undulations of the vortex shedding frequency component in the signal traces of $\theta = 80$ and 90 deg are out of phase essentially, inferring that the two measured locations were situated upstream and downstream of the flow separation point, respectively.

The preceding observations enlighten the unsteady nature of flow separation occurred on the circular cylinder. Basically, the unsteady characteristics are featured with two time scales, one of which is associated with the frequency of vortex shedding, and the other is much longer associated with the excursion of flow separation point in a circumferential extent, say, about 5 deg in the present case. It is interesting to point out that the preceding findings are in good agreement with the flow visualization results presented in Fig. 1, that the flow separation point is wandering around $\theta = 85$ deg. Note that the Reynolds numbers of the present study and the water-channel experiment mentioned previously are comparable.

In addition to the preceding findings learned with eye observations on the signal traces, the Wavelet analysis was carried out at each measured location to obtain the percentage of time during which the vortex shedding frequency was discernible. The criterion was defined to examine if a f_s value could be found within an interval of $F_s \pm 0.15F_s$ or not. As a result, the percentage values obtained at

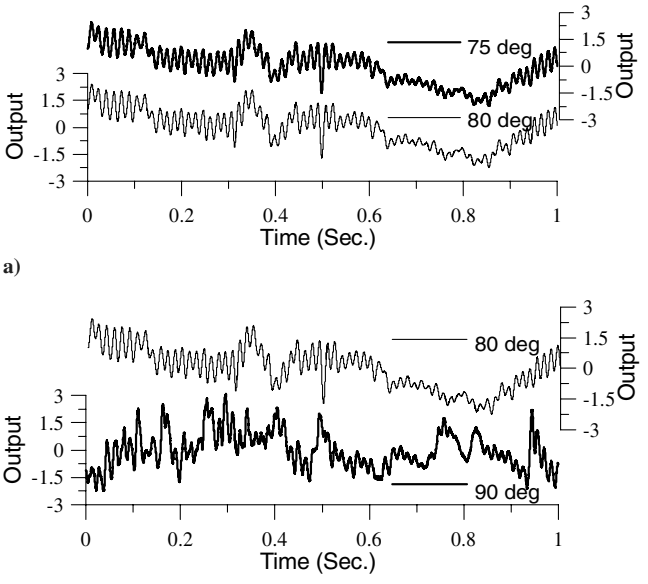

Fig. 8 Comparisons of the signal traces obtained at a) $\theta = 75$ and 80 deg, and b) $\theta = 80$ and 90 deg, for $Re = 1.65 \times 10^4$.

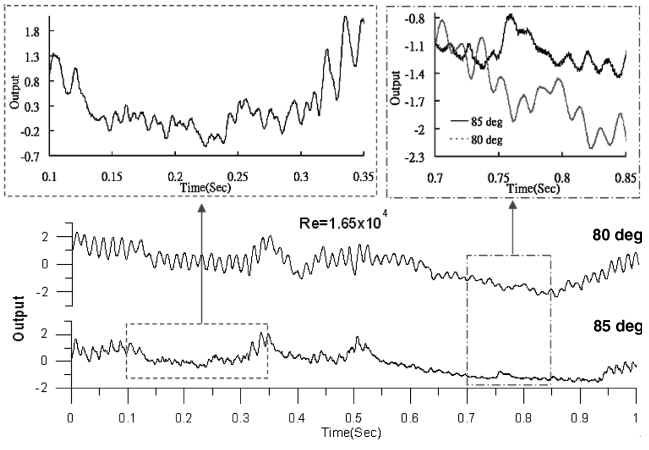

Fig. 7 A comparison of the signal traces measured on the cylinder surface.

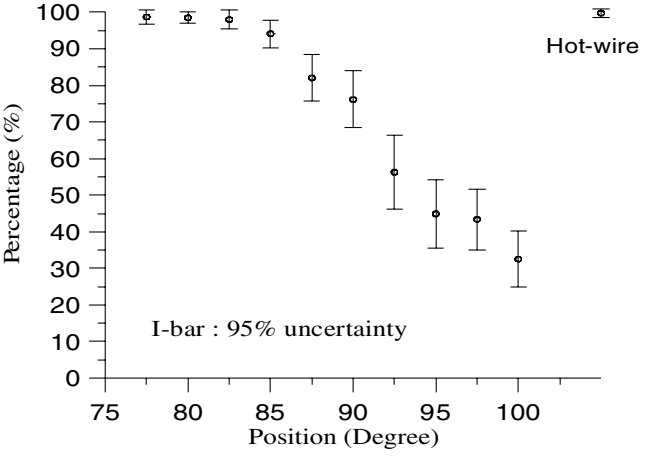

Fig. 9 Circumferential distribution of the percentage of time during which f_s was discernible with the present analysis.

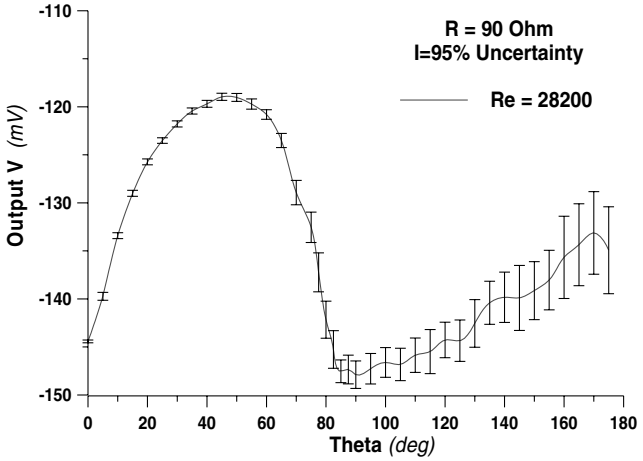

Fig. 10 Circumferential distribution of the time-mean voltage output of a MEMS sensor with the cold resistance 90 ohms on the circular cylinder, at $Re = 2.82 \times 10^4$.

$\theta = 77.5$–100 deg, $Re = 1.65 \times 10^4$, are presented in Fig. 9. Note that each data point shown in the figure indicates the mean of 21 values, each of which was reduced from a sampled record of 1.3 s. Together with each data point shown, the error bars indicate the 95% confidence interval associated with the mean value [18]. At $\theta = 77.5$–82.5 deg, the percentage values obtained appear very close to 100%, but not 100% exactly. This is because of the dropout events resulted in the present analysis, mentioned earlier. Also included in this plot for reference is the result reduced from the hot-wire signals obtained at $(x, y, z) = (1D, 1D, 0)$, which shows very close to 100% as well. At $\theta = 85$ deg, the percentage value appears to be lower somewhat. This is explained due to the fact mentioned earlier that the flow separation point is wandering in the neighborhood of this location. Referring to Achenbach [17], for the Reynolds numbers of 10^4 in the subcritical regime, the time-mean separation point on a circular cylinder was found slightly downstream of $\theta = 80$ deg. In an earlier study [19], the present authors examined the time-mean output of a MEMS sensor situated at various circumferential locations, and found that the lowest voltage value measured was in the neighborhood of $\theta = 82$ deg, which subsequently was referred to as the time-mean separation point. For reference, the results obtained by Tu et al. [19] at $Re = 2.82 \times 10^4$ are reproduced in Fig. 10. In the figure, the error bars shown with each data point indicate the 95% confidence interval. As noticed, downstream of $\theta = 82$ deg, the 95% confidence intervals get larger with θ, signifying the unsteadiness of flow in the separation region. In Fig. 9, it is also seen that in the region of $\theta = 85$–100 deg the 95% confidence intervals associated with the time-mean percentage values get larger downstream. These findings are noted to complement each other. In Fig. 9, the averaged percentage values get decreased monotonically from $\theta = 85$ to 100 deg. At $\theta = 100$ deg, the value is about 30%.

Physical Significance of Temporal Variations of Vortex Shedding Frequency

Physical significance inferred by the temporal variations of the f_s values seen in the region upstream of the separation point is further considered here. Referring to Fig. 6a, temporal variations of the f_s values appear irregular in time, which are featured with a characteristic time scale of 0.1 s, roughly speaking. Note that such a time scale is one order of magnitude greater than the time-mean vortex shedding period, which is about 0.016 s in this case.

Special attention could be paid to a large-scale variation of the f_s values around $t = 0.6$ s in Fig. 6a, which persists over a time length about 0.2 s. During the time, the f_s values appear substantially lower. Meanwhile, it is noted in Fig. 3 that during the time the fluctuating amplitudes of the signal traces of $\theta = 70$–85 deg appear substantially larger than those seen at the neighboring time instants. Moreover, the output levels of the signal traces appear to be higher compared with those at the neighboring time instants. Similarly, in Fig. 6a, during $t = 1.2$–1.6 s, the f_s values of $\theta = 70$–85 deg appear comparatively lower; meanwhile in Fig. 3 the signal traces consistently show that the fluctuating amplitudes are larger and the output levels are higher. Hence, a tendency learned from the preceding observations is that as the fluctuating amplitude of the vortex shedding frequency component in the raw signals gets larger, accompanied by higher output level, the f_s value tends to be lower. In examining the signals obtained by the thermal-film sensors on a cylinder, Blevins [4] pointed out that the larger the amplitude of the vortex shedding frequency component, the lower the frequency. In studying the temporal variations of the vortex shedding frequency reduced from the hot-wire signals measured in the wake of flow over a normal plate, Miau et al. [11] pointed out that larger amplitude of vortex shedding frequency component implied a situation that the separation vortex grew to a larger size before shedding. In this situation, the vortex shedding frequency value tended to be lower. These findings in the literature actually complement the present observations.

Quantitative evidence supporting the preceding observations is given in Table 3, in which the correlation coefficients of f_s and its modulus reduced from the signals of the hot wire at $(x, y, z) = (1D, 1D, 0)$ and the thermal film at $\theta = 70$ deg, in every 10 s, are presented. The hot-wire and hot-film signals were sampled at a rate of 1000 per second for 300 s. As seen, the correlation coefficients obtained fall in a range between -0.4 and -0.3. That the correlation coefficients appear negative indicates a trend that the larger the amplitude (modulus) of the vortex shedding frequency component, the lower the frequency f_s. Moreover, it is interesting to point out that the correlation coefficients shown in the table are comparable to those reported by Wu et al. [12], who performed the correlation between the vortex shedding frequency and its modulus of hot-wire signals obtained in the freestream of a wake behind a normal plate.

A further remark is made here concerning the appearance of the thermal-film sensor signals in Fig. 3 in the region upstream of flow separation. The signal traces show higher voltage output when larger amplitude of the vortex shedding frequency component takes place. Following previous discussion on heat transfer of a thermal film situated on the substrate, the appearance of high output level lasting over a considerable length of time infers a possibility of not only the thermal sensor but also the substrate giving heat to the flow. To gain better understanding of such a situation, further experiment was conducted with a normal hot wire situated very close to the surface at $\theta = 75$ deg. The probe was positioned in the boundary layer, for its mean output voltage was substantially lower than that measured in the freestream. Figure 11 presents the hot-wire and thermal-film signals obtained over a time period of 1 s, at $Re = 1.7 \times 10^4$, for

Table 3 Correlation coefficients obtained in every ten seconds between f_s and its modulus of the film sensor and hot-wire signals

Initial time instant, s	$T = 0$		$T = 60$		$T = 120$		$T = 180$		$T = 240$	
	Hot wire	Film	Hot wire	Film	Hot wire	Film	Hot wire	Film	Hot wire	Film
$t = T + 0$	−0.293	−0.258	−0.403	−0.405	−0.315	−0.357	−0.414	−0.436	−0.381	−0.333
$t = T + 10$	−0.460	−0.464	−0.285	−0.288	−0.341	−0.322	−0.326	−0.339	−0.346	−0.380
$t = T + 20$	−0.235	−0.257	−0.214	−0.252	−0.209	−0.203	−0.274	−0.272	−0.400	−0.408
$t = T + 30$	−0.374	−0.339	−0.291	−0.327	−0.326	−0.291	−0.183	−0.223	−0.348	−0.316
$t = T + 40$	−0.315	−0.306	−0.386	−0.359	−0.338	−0.310	−0.395	−0.325	−0.321	−0.289
$t = T + 50$	−0.384	−0.354	−0.373	−0.324	−0.259	−0.264	−0.272	−0.310	−0.278	−0.261

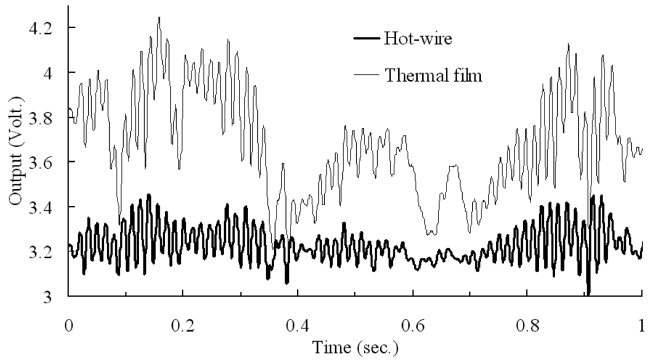

Fig. 11 Comparison of the thermal-film signals measured at $\theta =$ 75 deg and the hot-wire signals measured.

comparison. As seen, the fluctuations embedded in the hot-wire signal trace are dominated by the vortex shedding frequency component, which appear to correlate strongly with the fluctuations in the thermal-film trace. On the other hand, it is noted that the dc level of the hot-wire signal trace does not vary with time so much as that of the thermal-film signal trace. This appearance infers that the mean flow velocity at the point measured by the hot-wire probe did not vary significantly with time. Based on this observation, it is further speculated that the drift of the thermal-film output during a large-scale variation could be due to additional heat transfer from the substrate. Nevertheless, clarification of this issue is necessary in the future.

Conclusions

By applying Wavelet analysis with the signals measured by a MEMS sensors array flushed with a circular cylinder, substantial understandings were obtained regarding the unsteady characteristics of flow near the cylinder surface. The major findings are summarized next.

As revealed by the film sensor signals obtained at $\theta = 85$ deg, the unsteady behavior of flow separation was characterized by two time scales mainly, one of which was associated with vortex shedding, and the other was at least one order of magnitude longer, which was associated with the separation point wandering over a circumferential region of 5 deg roughly.

Wavelet analysis of the thermal-film signals obtained in the region of $\theta = 70$–80 deg, i.e., upstream of flow separation, indicated that the vortex shedding frequency could be discerned all the time. In the region of $\theta = 85$–100 deg, the percentage of time during which the vortex shedding frequency was discernible got decreased monotonically to about 30%. It was also confirmed that undulations of the vortex shedding frequency component seen in the signals measured upstream and downstream of flow separation were out of phase essentially.

Low-frequency modulations were noticed in the signals of the thermal-film sensors situated in the region upstream of flow separation and a hot wire in the freestream. The Wavelet analysis with these signals further indicated that the f_s value and its modulus reduced were correlated. The correlation coefficients fell in a range between -0.4 and -0.3. This finding infers a trend that the larger the amplitude of the vortex shedding frequency component, the lower the frequency f_s.

The present study illustrated a successful application of the MEMS thermal-film sensors together with the Wavelet analysis to unveil the unsteady characteristics of flow separation on a circular cylinder. It would be of interest to apply this experimental technique to study the flow separation phenomena of other bluff-body configurations in the future.

Acknowledgment

Funding supports of National Science Council, under the contract number NSC 93-2212-E-006-053, and Defense Foundation for this work are gratefully acknowledged.

References

[1] Gidet, W. H., "Effect of Turbulence Level of Incident Air Stream on Local Heat Transfer and Skin Friction on a Cylinder," *Journal of the Aeronautical Sciences*, Vol. 18, No. 11, 1951, pp. 725–730, 766.

[2] Bellhouse, B. J., and Schultz, D. L., "Determination of Mean and Dynamic Skin Friction, Separation and Transition in Low-Speed Flow with a Thin-Film Heated Element," *Journal of Fluid Mechanics*, Vol. 24, Pt. 2, Feb. 1966, pp. 379–400.

[3] Dwyer, H. A., and McCroskey, W. J., "Oscillating Flow over a Cylinder at Large Reynolds Number," *Journal of Fluid Mechanics*, Vol. 61, Pt. 4, Dec. 1973, pp. 753–767.

[4] Blevins, R. D., "The Effect of Sound on Vortex Shedding from Cylinders," *Journal of Fluid Mechanics*, Vol. 161, Dec. 1985, pp. 217–237.

[5] Lee, T., "Investigation of Unsteady Boundary Layer Developed on a Rotationally Oscillating Circular Cylinder," *AIAA Journal*, Vol. 37, No. 3, 1999, pp. 328–336.

[6] Liu, W. P., and Brodie, G. H., "A Demonstration of MEMS-Based Active Turbulence Transitioning," *International Journal of Heat and Fluid Flow*, Vol. 21, Pt. 3, June 2000, pp.297–303.

[7] Rott, N., "Unsteady Viscous Flow in the Vicinity of a Stagnation Point," *Quarterly of Applied Mathematics*, Vol. 13, April 1956, pp. 444–451.

[8] Telionis, D. P., "Review-Unsteady Boundary Layers, Separated and Attached," *Journal of Fluids Engineering*, Vol. 101, March 1979, pp. 29–43.

[9] McCroskey, W. J., "Some Current Research in Unsteady Fluid Dynamics- the 1976 Freeman Scholar Lecture," *Journal of Fluids Engineering*, Vol. 99, March 1977, pp. 8–38.

[10] Williams, J. C., III, "Incompressible Boundary-Layer Separation," *Annual Review of Fluid Mechanics*, Vol. 9, 1977, pp. 113–144.

[11] Miau, J. J., Wu, S. J., Hu, C. C., and Chou, J. H., "Low-Frequency Modulations Associated with Vortex Shedding from Flow over Bluff Body," *AIAA Journal*, Vol. 42, No. 7, 2004, pp. 1388–1397.

[12] Wu, S. J., Miau, J. J., Hu, C. C., and Chou, J. H., "On Low-Frequency Modulations and Three-Dimensionality in Vortex Shedding Behind Flat Plates," *Journal of Fluid Mechanics*, Vol. 526, March 2005, pp. 117–146.

[13] Roshko, A., "On the Development of Turbulent Wakes from Vortex Streets," NACA Rept. 1191, 1954.

[14] Farge, M., "Wavelet Transforms and Their Applications to Turbulence," *Annual Review of Fluid Mechanics*, Vol. 24, 1992, pp. 395–457.

[15] Menendez, A. N., and Ramaprian, B. R., "The Use of Flush-Mounted Hot-Film Gauges to Measure Skin Friction in Unsteady Boundary Layers," *Journal of Fluid Mechanics*, Vol. 164, March 1985, pp. 439–459.

[16] Breuer, K., "MEMS Sensors for Aerodynamic Applications- the Good, the Bad (and the Ugly)," AIAA Paper 2000-0251, Jan. 2000.

[17] Achenbach, E., "Distribution of Local Pressure and Skin Friction around a Circular Cylinder in Cross-Flow up to $Re = 5 \times 10^6$," *Journal of Fluid Mechanics*, Vol. 34, Pt. 4, Dec. 1968, pp. 625–639.

[18] Bendat, J. S., and Piersol, A. G., *Random Data Analysis and Measurement Procedure*, 2nd ed., John Wiley & Sons, Singapore, 1991.

[19] Tu, J. K., Miau, J. J., Chou, J. H., and Lee, G. B., "A Flexible Skin with Arrayed Temperature Sensors and its Applications for Detection of Separation Points," *Proceedings of the 19th Annual Meeting of Chinese Society of Mechanical Engineers (CSME)*, National Huwei Institute of Science and Technology, Huwei, Taiwan, 2002, pp. 849–855.

R. Lucht
Associate Editor